

Intramolecular Energy Transfer to *trans*-Stilbene[†]

Kirk S. Schanze,* Lucian A. Lucia, Megan Cooper, Keith A. Walters, Hai-Feng Ji, and Osvaldo Sabina

Department of Chemistry, University of Florida, Gainesville, Florida 32611-7200

Received: November 13, 1997; In Final Form: January 13, 1998

This study examines the photophysics of a series of transition-metal complexes that contain a (diimine)Re^I-(CO)₃(py) chromophore covalently linked to *trans*-stilbene via a semirigid amide spacer. In this series of complexes moderately exothermic triplet–triplet energy transfer from the ³dπ* charge-transfer excited state of the diimine–Re chromophore to *trans*-stilbene is competitive with “normal” radiative and nonradiative decay of the ³dπ* state. The rate constant for intramolecular energy transfer (*k*_{ENT}) was determined as a function of temperature from 190 to 290 K for three complexes in which the driving force (Δ*E*_{ENT}) varies from ca. –29 to –38 kJ mol^{–1}. The temperature-dependence data indicate that energy transfer is characterized by a low activation energy (*E*_a ≤ 2 kJ mol^{–1}) and a low-frequency factor (*A* ≈ 10⁶ s^{–1}). The results are interpreted by a mechanism in which energy transfer from the ³dπ* state to *trans*-stilbene occurs at nearly the optimal driving force (i.e., Δ*E*_{ENT} ≈ λ, where λ is the reorganization energy). However, owing to the moderate separation distance between the Re(I) center and *trans*-stilbene, the exchange coupling matrix element (*V*_{TT}) is small, leading to low *A* values.

Introduction

It has long been recognized that *cis*-stilbene is an unusual acceptor of triplet excitation energy. Hammond and co-workers first reported that *cis*-stilbene accepts excitation energy from triplet donors at rates significantly greater than predicted when the donors have triplet energies less than the spectroscopic energy of the *cis*-stilbene triplet.^{1–4} This observation for *cis*-stilbene has been confirmed by more recent studies and has also been reported for other triplet acceptors that contain flexible π-electron systems.^{5–8} Unusually rapid endothermic energy transfer to acceptors with flexible π-systems has been termed “nonvertical” energy transfer.^{2,4} Nonvertical energy transfer is believed to involve the production of an excited-state acceptor having a geometry that is different from that of the relaxed ground-state olefin. The geometrically distorted nonvertical excited state lies at lower energy than the state produced by a vertical (spectroscopic) transition and therefore is populated by triplet donors having insufficient energy to populate the vertical excited state.² Nonvertical energy transfer is believed to arise because the Franck–Condon restrictions that hold for (vertical) spectroscopic transitions are relaxed owing to the comparatively long donor–acceptor interaction times that are involved in energy transfer.

Saltiel and co-workers examined the temperature dependence of the rate of endothermic intermolecular energy transfer from low-energy triplet donors to *cis*- and *trans*-stilbene.^{9,10} They found that for both isomers endothermic energy transfer is characterized by a relatively low activation enthalpy (Δ*H*[‡]) and a large negative activation entropy (Δ*S*[‡]).¹⁰ Moreover, when activation parameters for energy transfer to the stilbene isomers are compared for two low-energy triplet donors, the energy deficit for the lower-energy donor is not reflected by an increase in Δ*H*[‡] as predicted by the Sandros equation,^{11,12} but rather by

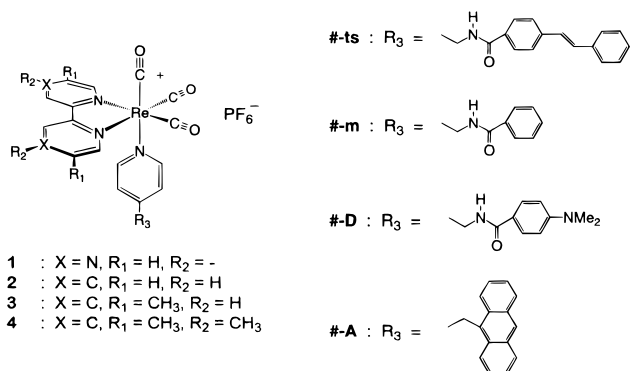
a larger negative Δ*S*[‡] (i.e., Δ*H*[‡] remains constant irrespective of the donor triplet energy). Saltiel suggested that deviation of the experimental activation parameters from the behavior predicted by the Sandros equation is due to the fact that nonvertical energy transfer occurs for *both* stilbene isomers.¹⁰ A model was presented that suggested that nonvertical energy transfer involves a transition state in which the stilbene acceptor assumes a geometry that is twisted with respect to the C=C bond, thereby decreasing the energy demands on the triplet donor. In more recent work, Gorman and Caldwell propose that nonvertical energy transfer only occurs to *cis*-stilbene.¹³ These authors further suggest that the role of C=C bond twisting in nonvertical energy transfer is minimal and that the dominant mode that is active in the transition state for nonvertical energy transfer is phenyl–vinyl torsion.¹³

Transition-metal complexes of the type (b)Re^I(CO)₃(L) feature long-lived, low-energy excited states based on a d(Re) → π* (NN) charge-transfer transition (b = a diimine ligand such as 2,2′-bipyridine). By analogy to the lowest dπ* charge-transfer states in trisdiimine complexes of Ru(II), the dπ* state in the diimine–Re(I) complexes has a large degree of triplet spin character and thus can be referred to as ³dπ*.¹⁴ Consistent with the triplet spin assignment, excited-state (b)Re^I(CO)₃(L) complexes serve as triplet-energy donors. Thus, early work by Wrighton and co-workers demonstrated bimolecular diffusion-controlled energy transfer from a series of (b)Re^I(CO)₃Cl complexes to several organic triplet acceptors including *trans*-stilbene.^{15,16}

More recently, our group employed the (b)Re^I(CO)₃(L) chromophore to investigate the kinetics of intramolecular energy and electron transfer.^{17–20} These studies take advantage of the fact that the energy and reduction potential of the ³dπ* state can be “tuned” by varying the electronic demand of the diimine ligand, which serves as the acceptor for the dπ* charge-transfer transition. In the course of this work we have examined the

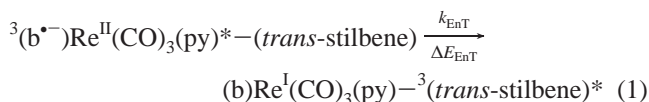
[†] Dedicated to Professor Jack Saltiel on the occasion of his 60th birthday.

driving-force dependence of photoinduced electron transfer in **1-D**, **2-D** and **4-D** and of triplet-triplet energy transfer in **1-A**–**3-A** (see structures).^{17,18} This work clearly demonstrates the



utility of the ³dπ* excited state in exploring correlations between the thermodynamics and kinetics of energy and electron transfer.

An interest in the stilbene energy-transfer problem, coupled with our experience with intramolecular energy and electron transfer in the (b)Re^I(CO)₃(L) system, led us to synthesize and examine the photophysical properties of the series of complexes **1-ts**–**4-ts**. This series of covalently linked Re–stilbene complexes was designed to allow investigation of the driving-force dependence of energy transfer from the ³dπ* state of the diimine–Re(I) chromophore to *trans*-stilbene, that is,



where k_{EnT} and ΔE_{EnT} are, respectively, the rate constant and driving force for energy transfer. We believed that it would be possible to obtain additional information concerning the mechanism of triplet-energy transfer to *trans*-stilbene by examining the temperature dependence of k_{EnT} as a function of the energy of the ³dπ* state of (b)Re^I(CO)₃(L). Re–stilbene complexes **1-ts**–**4-ts** have an advantage over the bimolecular systems studied previously because the donor and acceptor are covalently linked, which alleviates the need to correct for the kinetics of diffusion.

The present manuscript describes a photochemical and photophysical investigation of **1-ts**–**4-ts**. The results of this investigation indicate that when the energy of the ³dπ* state of the diimine–Re chromophore exceeds ca. 209 kJ mol⁻¹, intramolecular energy transfer to *trans*-stilbene occurs. The temperature dependence of the rate of intramolecular energy transfer was determined from 190 to 290 K, and the results indicate that energy transfer is characterized by a low activation energy (E_a) and a low frequency factor (A). The results are interpreted by a mechanism in which energy transfer from the ³dπ* state to *trans*-stilbene occurs at nearly the optimal driving force (i.e., $\Delta E_{\text{EnT}} \approx \lambda$). However, owing to the moderate separation distance between the Re(I) center and *trans*-stilbene, the exchange coupling matrix element is small (V_{TT}), which gives rise to the low A value.

Experimental Section

Synthesis. Model complexes **1-m**–**4-m** were available from a previous study. The *trans*-stilbene-substituted complexes **1-ts**–**4-ts** were prepared from the corresponding (b)Re(CO)₃Cl complexes (b = 2,2'-bipyridine, 2,2'-bipyridine, 5,5'-dimethyl-2,2'-bipyridine and 4,4',5,5'-tetramethyl-2,2'-bipyridine) and the

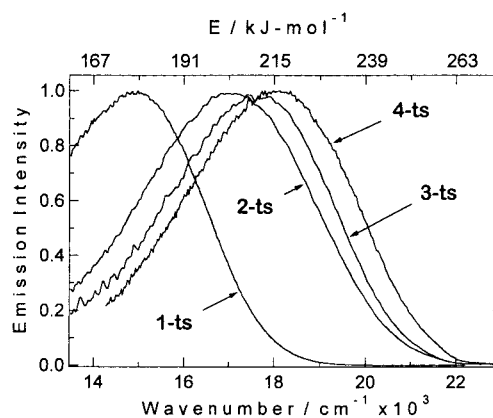


Figure 1. Emission spectra of *trans*-stilbene-substituted complexes in CH₃CN solution ($\lambda_{\text{ex}} = 350$ nm).

substituted pyridine ligand *trans*-*N*-(4-aminomethylpyridyl)-4-stilbene carboxamide (**5**) according to a literature procedure.¹⁷ The complexes were purified by column chromatography on silica gel. The ¹H NMR and ¹³C NMR spectra of **1-ts**–**4-ts** are in accord with their structures. Sample purity was further established by elemental analysis. **1-ts**. Anal. Calcd for C₃₂H₂₄F₆N₆O₄PRE: C, 43.29; H, 2.72; N, 9.46. Found: C, 40.67; H, 2.54; N, 8.68. **2-ts**. Anal. Calcd for C₃₄H₂₆F₆N₄O₄PRE: C, 46.10; H, 2.96; N, 6.33. Found: C, 45.69; H, 3.09; N, 6.06. **3-ts**. Anal. Calcd for C₃₆H₃₀F₆N₄O₄PRE: C, 47.32; H, 3.31; N, 6.13. Found: C, 47.59; H, 3.41; N, 6.07. **4-ts**. Anal. Calcd for C₃₈H₃₄F₆N₄O₄PRE: C, 48.46; H, 3.64; N, 5.95. Found: C, 48.05; H, 4.03; N, 6.18.

Photochemistry and Photophysics. The samples used for steady-state experiments were degassed by bubbling with Ar for 20–30 min. Samples used for variable-temperature emission-lifetime experiments were freeze–pump–thaw–degassed four times and sealed in Pyrex tubes under high vacuum. Corrected steady-state emission spectra were recorded on a SPEX F-112 fluorometer. Emission lifetimes were determined by time-correlated single-photon counting on a commercially available instrument (PRA) that relies on an H₂-filled spark discharge as the excitation source. Excitation and emission wavelengths were selected by using band-pass filters (excitation, Schott UG-11; emission, 550- or 600-nm interference filter). Lifetimes were calculated by using the DECAN deconvolution software on a 486 PC.²¹ Low-temperature lifetimes were obtained by cooling the samples in an Oxford Instruments DN-1704 optical cryostat. The acetonitrile and butyronitrile solvents were distilled prior to use.

Steady-state photochemical experiments were carried out by using the 366-nm output from a 75-W high-pressure Hg arc lamp that is housed in an elliptical reflector housing (PTI, ALH-1000). The photolysis beam was passed through a grating monochromator and focused onto a 1 cm × 1 cm quartz cell that contained 3 mL of the sample solution and a magnetic stirrer. Samples were exposed to light for a short period of time, and then the UV–visible absorption spectrum was measured on an HP 8450A diode-array spectrophotometer.

Results

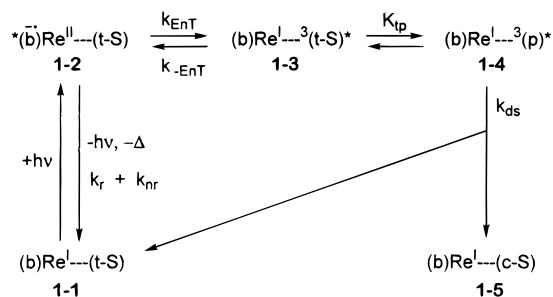
Figure 1 illustrates the ³dπ* emission spectra (intensity normalized) for **1-ts**–**4-ts**, and Table 1 lists the emission-band maxima and onset energies. Model complexes **1-m**–**4-m**, which do not contain the *trans*-stilbene chromophore, feature emission spectra that are identical in energy and band shape with those of the corresponding *trans*-stilbene analogues. Figure

TABLE 1: Photophysical Properties of Re–Stilbene Complexes^a

complex	E_{\max}/cm^{-1} (kJ mol ⁻¹)	$E_{\text{onset}}/\text{cm}^{-1}$ (kJ mol ⁻¹)	$E_{\text{d}\tau^*}/\text{kJ mol}^{-1}$ ^c	$\Delta E/\text{kJ mol}^{-1}$	$\tau_{\text{em}}/\text{ns}$	$k_{\text{obs}}/\text{s}^{-1}$	η_{obs}
1-ts	14 900 (178)	17 900 (214)	192 ± 17	0	28.4	<10 ⁶	0
1-m					28.0		
2-ts	17 065 (204)	20 700 (247)	222 ± 17	-29	191	6.0 × 10 ⁵	0.11
2-m					216		
3-ts	17 760 (210)	20 900 (250)	226 ± 17	-33	363	1.6 × 10 ⁶	0.58
3-m					860		
4-ts	18 100 (216)	21 400 (256)	230 ± 17	-38	615	6.4 × 10 ⁵	0.39
4-m					1015		

^a All data for 70% *n*-BuCN/CH₃CN solvent at 290 K. ^b E_{onset} taken as point on high-energy side of band where $I = 0.1I_{\text{max}}$. ^c $E_{\text{d}\tau^*}$ is average of E_{max} and E_{onset} .

SCHEME 1



1 reveals that the energy of $^3\text{d}\tau^*$ decreases along the series **4-ts** > **3-ts** > **2-ts** \gg **1-ts**. The trend in energy reflects the effect of the substituents on the π^* (LUMO) energy of the diimine ligand, which serves as the acceptor for the $\text{d}\tau^*$ charge-transfer transition.

Lifetimes for the $^3\text{d}\tau^*$ emission at room temperature (τ_{em}) were determined for **1-ts**–**4-ts** and **1-m**–**4-m** (Table 1). In all cases the emission decays were single exponential (i.e., first-order kinetics). For the model complexes, the lifetimes reflect the “natural” decay rate of $^3\text{d}\tau^*$ via radiative and nonradiative pathways (k_r and k_{nr} , Scheme 1). It is clear that τ_{em} decreases along the series **4-m** > **3-m** > **2-m** \gg **1-m**. The variation in τ_{em} implies that the nonradiative-decay rate constant (k_{nr}) increases as the energy of $^3\text{d}\tau^*$ decreases.²² This effect, termed the “energy-gap law”, has been documented for a wide variety of d^6 transition-metal polypyridine complexes, including those based on $\text{Re}(\text{I})$.^{23–25} Interestingly, the τ_{em} values for *trans*-stilbene-substituted complexes **2-ts**–**4-ts** are smaller than for the corresponding model complexes; however, τ_{em} is the same within experimental error for **1-m** and **1-ts**. This result indicates that for **2-ts**–**4-ts** an additional excited-state decay pathway operates, and as outlined below, we believe that the accelerated emission decay is due to intramolecular energy transfer (eq 1).

Under the assumption that the stilbene chromophore does not affect k_r and k_{nr} for the $^3\text{d}\tau^*$ state, the energy-transfer rate constant (k_{obs}) and the efficiency of energy transfer (η_{obs}) can be calculated by the following equations:

$$k_{\text{obs}} = 1/\tau_{\text{ts}} - 1/\tau_{\text{m}} \quad \eta_{\text{obs}} = 1 - (\tau_{\text{ts}}/\tau_{\text{m}}) \quad (2)$$

where τ_{ts} and τ_{m} are the emission lifetimes of corresponding model and *trans*-stilbene complexes. Values of k_{obs} and η_{obs} for the *trans*-stilbene complexes are collected in Table 1. The experimental data suggest that at room temperature the rate of energy transfer in **2-ts**, **3-ts**, and **4-ts** is approximately constant ($k_{\text{obs}} \approx 10^6 \text{ s}^{-1}$). However, because the $^3\text{d}\tau^*$ state is longer-lived in **3-ts** and **4-ts**, the efficiency of energy transfer (η_{obs}) is larger for these complexes. The emission lifetime is approximately the same for **1-m** and **1-ts**, which implies that intramolecular energy transfer is too slow to compete with

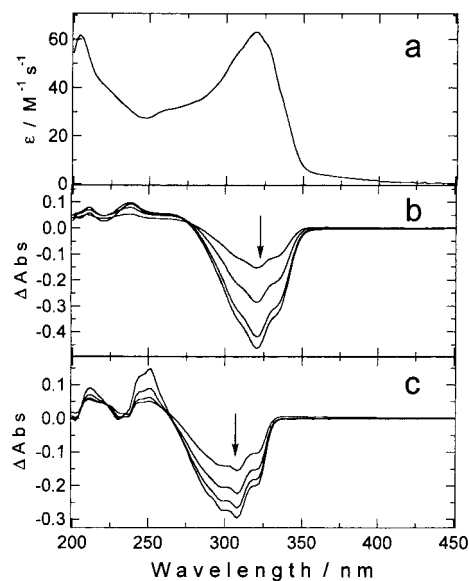


Figure 2. (a) UV–visible absorption of **2-ts** in CH₃CN solution. (b) UV–visible difference absorption spectra ($\Delta\text{Abs} = A_t - A_{t=0}$) of a solution of **2-ts** in CH₃CN as a function of photolysis time ($\lambda = 366$ nm; 2, 4, 10, and 20 min). (c) UV–visible difference absorption spectra ($\Delta\text{Abs} = A_t - A_{t=0}$) of a solution of free-ligand **5** in CH₃CN as a function of photolysis time ($\lambda = 313$ nm; 2, 4, 10, and 20 min).

radiative and nonradiative decay of the $^3\text{d}\tau^*$ state in the latter complex. Nonetheless, the fact that τ_{em} is the same for **1-ts** and **1-m** provides evidence that the stilbene chromophore does not influence k_r and k_{nr} for the $^3\text{d}\tau^*$ state.

Evidence supporting the occurrence of energy transfer from the $^3\text{d}\tau^*$ state to *trans*-stilbene is provided by steady-state photochemical experiments carried out on **1-ts**–**3-ts** and the free ligand *trans*-*N*-(4-aminomethylpyridyl)-4-stilbene carboxamide (**5**).²⁶ Figure 2a illustrates the absorption spectrum of **2-ts**. This spectrum is dominated by the π, π^* absorption of the *trans*-stilbene chromophore which has $\lambda_{\text{max}} \approx 320$ nm. The $\text{d}\tau^*$ absorption of the bpy-Re chromophore appears as a “tail” extending from 350 nm into the visible region. Figure 2b illustrates difference absorption spectra of a solution of **2-ts** obtained following photolysis into the $\text{d}\tau^*$ absorption band at 366 nm. Photolysis bleaches the π, π^* absorption of the *trans*-stilbene chromophore and induces a small increase in absorption in the 200–300-nm region. Similar absorption changes are observed when free-ligand **5** is photolyzed at 313 nm (Figure 2c). The spectral changes observed concomitant with photolysis of **2-ts** and **5** are consistent with the occurrence of *trans* \rightarrow *cis* photoisomerization of the stilbene chromophore.²⁷ It is significant that photoisomerization occurs in **2-ts** even though 366-nm light is absorbed exclusively by the bpy-Re chromophore. This observation provides compelling evidence that $^3\text{d}\tau^* \rightarrow ^3\pi, \pi^*$ intramolecular energy transfer occurs (eq 1).

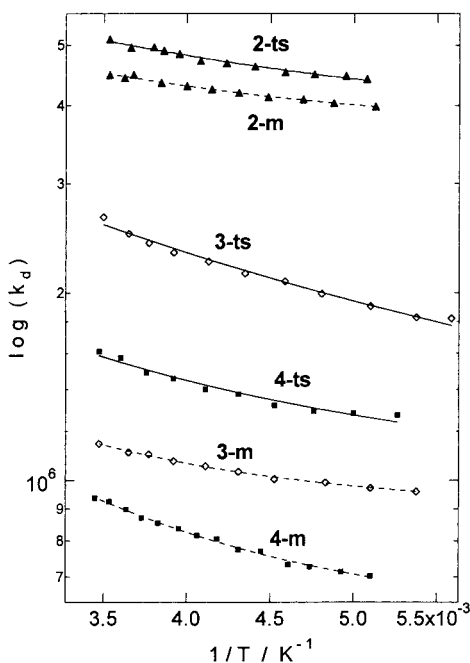


Figure 3. Plots of $\log(k_d)$ vs inverse T for **2-m-4-m** and **2-ts-4-ts** (where $k_d = 1/\tau_{em}$). Symbols mark experimental data. Lines through data for **2-m-4-m** and **2-ts-4-ts** were calculated by using eqs 4 and 5, respectively.

Further evidence linking the emission-lifetime quenching in the *trans*-stilbene complexes to intramolecular energy transfer comes from a comparison of the relative efficiency for photoisomerization in **1-ts-3-ts**. Thus, photolysis of **2-ts** at 366 nm ($[2-ts] = 2 \times 10^{-5}$ M, $I_{hv} 1 \times 10^{-8}$ ein s $^{-1}$) induces a decrease in the absorption at 320 nm at an initial rate of $k = 0.00048$ s $^{-1}$. The same experiment carried out on **3-ts** leads to $k = 0.0016$ s $^{-1}$. By contrast, photolysis of **1-ts** for an extended period leads only to a small decrease in the absorption at 320 nm. Interestingly, photoisomerization occurs at an initial rate that is approximately 3.3 times faster for **3-ts** than for **2-ts**. This difference is qualitatively in accord with the emission-lifetime data, which suggest that intramolecular energy transfer is 5 times more efficient in **3-ts** than in **2-ts**. Moreover, the fact that photolysis of **1-ts** does not effect photoisomerization is consistent with the equivalence of τ_{em} in this complex and **1-m** and demonstrates that energy transfer is very inefficient in **1-ts**.

To provide detailed information concerning the temperature dependence of the energy-transfer rate, emission lifetimes of **2-m-4-m** and **2-ts-4-ts** were determined as a function of temperature from 190 to 290 K in a butyronitrile–acetonitrile solvent mixture (7:3 v/v). For all of the complexes over the entire temperature range the emission decays were first-order. Figure 3 illustrates plots of the experimental data (as $\log k_d$ vs $1/T$, where $k_d = 1/\tau_{em}$ and T is absolute temperature). Over the entire temperature range the decay rates of **2-ts-4-ts** are greater than those of the corresponding model complexes (**2-m-4-m**), which suggests that energy transfer occurs for all of the complexes over the 190–290 K range.

Discussion

The available experimental data provide strong evidence that in **2-ts-4-ts** excitation of the metal–complex-based $^3d\pi^*$ excited state leads to intramolecular energy transfer to the *trans*-stilbene chromophore as shown in eq 1. Intramolecular energy transfer does not occur in bipyrazine complex **1-ts**; in this case the rate of energy transfer is too low to effectively compete

with decay of the $^3d\pi^*$ state by normal pathways. We now consider the various aspects of the photophysics of the *trans*-stilbene complexes to obtain quantitative information concerning the mechanism of intramolecular energy transfer.

Energetics of Energy Transfer. One objective of the present study is to examine the relationship between the driving force and the dynamics of intramolecular energy transfer from the $^3d\pi^*$ state to the $^3\pi,\pi^*$ state of *trans*-stilbene. To determine the driving force for this process, one may apply the relationship

$$\Delta E_{EnT} = E_{t-s} - E_{d\pi^*} \quad (3)$$

where E_{t-s} is the triplet energy of the *trans*-stilbene chromophore and $E_{d\pi^*}$ is the energy of the $^3d\pi^*$ state in complexes **1-ts-4-ts**. Phosphorescence spectroscopy indicates that the triplet energies of *trans*-stilbene and *trans*-4-acetylstilbene are 205 and 180 kJ mol $^{-1}$, respectively.^{28,29} Unfortunately, $^3\pi,\pi^*$ phosphorescence from the stilbene chromophore was not observed at 77 K from the metal complexes **1-ts-4-ts** or from free-ligand **5** in the presence of ethyl iodide. However, the triplet energy of *trans*-4-acetylstilbene likely provides a close approximation for E_{t-s} in the Re–stilbene complexes, and therefore, $E_{t-s} = 180$ kJ mol $^{-1}$ is used in the calculations of ΔE_{EnT} .

Despite the fact that emission is clearly observed from the $^3d\pi^*$ state of the diimine–Re(I) chromophore in **1-ts-4-ts**, it is difficult to pinpoint the energy of the relaxed $^3d\pi^*$ state because the emission band is broad and structureless. A variety of approaches have been used to determine the thermally averaged energies of the relaxed $d\pi^*$ state in transition-metal complexes ($E_{d\pi^*}$), including estimates based on the difference between S \rightarrow T absorption- and emission-band maxima,³⁰ Franck–Condon band-shape analysis (i.e., emission spectral fitting),^{24,25} and pulsed photocalorimetry.³¹ Each approach has its merits and disadvantages; however, perusal of the (extensive) literature data suggests that a very good approximation for $E_{d\pi^*}$ is obtained by taking the average of the emission band onset and the emission band energy. Table 1 lists energies for the emission maxima, emission onset and values of $E_{d\pi^*}$ for **1-ts-4-ts** estimated by averaging the band-onset and maximum energies. Using these values and E_{t-s} in eq 3 leads to the estimates for ΔE_{EnT} that are also compiled in Table 1. Note that energy transfer is moderately exothermic for **2-ts-4-ts** and is approximately thermoneutral for **1-ts**.

Excited-State Model and Kinetics of Energy Transfer. An important question that must be addressed concerns the relationship of the “observed” rate of intramolecular quenching (i.e., k_{obs} from eq 2) to the rate of intramolecular energy transfer (k_{EnT}). To address this point, it is necessary to consider all excited states that may be involved in the photophysics of *trans*-stilbene complexes **2-ts-4-ts**. In Scheme 1, **1-2** represents the $^3d\pi^*$ excited state of the diimine–Re chromophore, **1-3** is the *trans*-stilbene triplet, **1-4** is the twisted stilbene triplet, and **1-5** is the ground-state complex containing *cis*-stilbene. This scheme, which is based in part on extensive photochemical and photophysical studies of the stilbenes,^{4,27,32–35} has several features that are important to our model. (1) Energy transfer from the $^3d\pi^*$ state directly affords the *trans*-stilbene triplet (**1-2** \rightarrow **1-3**, rate = k_{EnT}). (2) In principle (see below), energy transfer may be reversible (**1-3** \rightarrow **1-2**, rate = k_{-EnT}). (3) The *trans*-triplet (**1-3**) exists in equilibrium with the twisted triplet (**1-4**); this equilibrium is established rapidly and favors the twisted triplet ($K_{ip} \approx 10$).³⁴ (4) The primary channel for decay is via the twisted triplet (**1-4**); flash-photolysis studies of a wide variety of substituted stilbenes indicate that the triplet lifetime is ~ 60 ns ($k_{ds} = 1.7 \times 10^7$ s $^{-1}$).³⁴

TABLE 2: Parameters from Emission Lifetime Temperature Dependence^a

complex	k_0/s^{-1}	A_1/s^{-1}	$E_a^1/kJ\ mol^{-1}$	A_2/s^{-1}	$E_a^2/kJ\ mol^{-1}$
2-m	3.6×10^6	5.6×10^6	4.2		
2-ts	3.6×10^6	5.6×10^6	4.2	1.4×10^6	2.1
3-m	9.0×10^5	3.3×10^6	6.3		
3-ts	9.0×10^5	3.3×10^6	6.3	3.7×10^6	2.1
4-m	5.9×10^5	4.2×10^6	5.9		
4-ts	5.9×10^5	4.2×10^6	5.9	9.0×10^5	0.8

^a Emission lifetimes obtained in 70% *n*-BuCN/CH₃CN over temperatures ranging from 190–290 K.

The important feature with respect to the present study is to relate the observed quenching rate of the ³dπ* state (**1-2**) (k_{obs} from eq 2) to the rate of energy transfer (k_{EnT}). Although a closed-form equation for the kinetics in Scheme 1 was not derived, a chemical-kinetics simulation program that relies on numerical integration was used to model Scheme 1.³⁶ This simulation demonstrated unequivocally that when $k_{ds} \gg k_{EnT}$ (which is the case for **2-ts–4-ts**), the decay rate of the ³dπ* state is equal to $k_r + k_{nr} + k_{EnT}$ (i.e., the observed rate derived from eq 2 is equal to the rate of energy transfer k_{EnT}). Quite interestingly, even when energy transfer is endothermic (and therefore energy transfer is reversible, $k_{-EnT} > k_{EnT}$), the simulation reveals that as long as $k_{ds} \gg k_{EnT}$, the rate of ³dπ* decay is equivalent to $k_r + k_{nr} + k_{EnT}$. In summary, the kinetics simulation of Scheme 1 provides strong support for the assumption that in **2-ts–4-ts**, $k_{EnT} \approx k_{obs} = 1/\tau_{ts} - 1/\tau_m$.

Analysis of Temperature-Dependent Rate Data. The temperature-dependent lifetime data were subjected to a thorough analysis in order to extract information concerning the Arrhenius parameters for energy transfer. First, the lifetime data for the model complexes were analyzed to account for the temperature dependence of the “normal” excited-state decay channels (k_r and k_{nr} , Scheme 1) by using eq 4,

$$k_d(T) = k_0 + A_1 \exp\{-E_a^1/(RT)\} \quad (4)$$

where $k_d(T)$ is the observed emission decay rate at each temperature ($k_d(T) = 1/\tau_{em}(T)$). This equation is based on a model in which the total decay rate of the ³dπ* excited state ($k_r + k_{nr}$, Scheme 1) is comprised of a temperature-independent component k_0 and a temperature-dependent component that is characterized by frequency factor and activation energy A_1 and E_a^1 , respectively.^{24,37,38} Table 2 contains the parameters extracted from nonlinear regression analysis of the temperature-dependence data for **2-m–4-m**, and the dashed lines in Figure 3 were calculated using eq 4 with these parameters. The observed temperature dependence of the lifetime of the ³dπ* state in **2-m–4-m** is similar to that observed in other d⁶ transition-metal–polypyridine complexes when there is *not* a ³dd excited state that is thermally accessible from the ³dπ* state.³⁹ In the present systems, the emission lifetime is weakly temperature-dependent; decay is characterized by a small activation energy (ca. 4 kJ mol⁻¹ for **2-m–4-m**) and a low frequency factor. In the context of currently accepted models of the excited-state dynamics d⁶ polypyridine complexes,^{14,37} the temperature-dependence data for **2-m–4-m** imply that the ³dπ* manifold consists of at least two emitting states that are separated by approximately 4 kJ mol⁻¹ (350 cm⁻¹).

The fact that the emission decay of model complexes **2-m–4-m** is weakly temperature-dependent signals that decay of the ³dπ* state via “normal” pathways is weakly activated. Therefore, to model the temperature dependence of the emission decay rate for the *trans*-stilbene complexes **2-ts–4-ts**, it is necessary

to use an expression that accommodates decay via *two* activated channels, that is, eq 5,

$$k(T) = k_0 + A_1 \exp\{-E_a^1/(RT)\} + A_2 \exp\{-E_a^2/(RT)\} \quad (5)$$

where A_1 , E_a^1 and A_2 , E_a^2 are, respectively, the frequency factors and activation energies for the first and second activated decay channels.^{20,40} When eq 5 was used to fit the emission-decay data for the *trans*-stilbene complexes (**2-ts–4-ts**), k_0 , A_1 and E_a^1 were fixed at the values determined by fitting the decays of the corresponding model complexes. Nonlinear regression was then used to fit the experimental temperature-dependence data by varying the remaining two parameters (A_2 and E_a^2). The results obtained from this analysis are listed in Table 2 and the solid lines in Figure 3 were calculated using eq 5 with the parameters listed in the table.

By analyzing the temperature dependence of the emission decay rates for **2-ts** and **4-ts** according to eq 5 with the constraints outlined in the preceding paragraph, we attempt to separate the activation parameters for the two excited-state decay channels available to the *trans*-stilbene complexes. Thus, we suggest that the first set of activation parameters (A_1 and E_a^1) corresponds to decay via the “normal” radiative and nonradiative channels and the second set corresponds to intramolecular energy transfer (i.e., $A_2 = A_{EnT}$ and $E_a^2 = E_a^{EnT}$, where A_{EnT} and E_a^{EnT} are the frequency factor and activation energy for energy transfer). Under the assumptions of this model, the A_2 and E_a^2 values recovered for **2-ts–4-ts** (Table 2) indicate that intramolecular energy transfer is nearly activationless ($E_a^2 < 2.1$ kJ mol⁻¹) and is accompanied by a very low frequency factor ($A_2 \approx 10^6$ s⁻¹).

Mechanism of Energy Transfer in the Re–Stilbene Complexes. The initial objective of this study was to examine endothermic intramolecular energy transfer to *trans*-stilbene. Thus, preliminary efforts were focused on a stilbene-substituted complex that has a low-energy ³dπ* excited state. Complex **1-ts** contains the 2,2'-bipyrazine acceptor ligand, which, because of its low reduction potential, affords a low-energy ³dπ* excited state.¹⁹ We believed that this complex would afford the opportunity to explore endothermic energy transfer to *trans*-stilbene. Unfortunately, the photophysical and photochemical studies indicate that in **1-ts** nonradiative decay from the ³dπ* state is too rapid to allow (thermoneutral) energy transfer to compete with excited-state decay.

The initial findings with **1-ts** led to the studies of **2-ts–4-ts**. In this series, the ³dπ* state is at a higher energy and intramolecular energy transfer to *trans*-stilbene is moderately exothermic. Although energy transfer occurs at measurable rates in **2-ts–4-ts** (Table 1), there is not a significant difference in the driving force for energy transfer (ΔE_{EnT}) among this series. The similarity in the driving force for energy transfer in **2-ts–4-ts** is reflected by the fact that the energy-transfer rates (and Arrhenius parameters) are the same within experimental error for the series. Because of the close spacing of ΔE_{EnT} in **2-ts–4-ts**, there is insufficient information to carry out a detailed analysis of the correlation between the activation parameters for energy transfer and ΔE_{EnT} . Nonetheless, a great deal of information is contained in the temperature-dependent rate data, and therefore, we turn our attention to analysis of this aspect of the study.

Classical and quantum-mechanical theories indicate that moderately exothermic Dexter exchange energy transfer processes will be activationless (i.e., when $\Delta E_{EnT} = \lambda$, $E_a \approx 0$).^{10,41–44} The temperature dependence data for **2-ts–4-ts** are consistent with the theoretical predictions—as mentioned above,

for these complexes energy transfer is moderately exothermic and k_{EnT} is nearly temperature-independent. However, despite the fact that energy transfer is activationless in **2-ts**–**4-ts**, the process remains comparatively slow. This points to the fact that in **2-ts**–**4-ts** the frequency factor for intramolecular energy transfer is low (A_2 , Table 2). To understand the origin of the low frequency factor, it is necessary to consider the theory of energy transfer in more detail.

In the quantum-mechanical approach, Dexter exchange energy transfer is treated as a nonradiative decay process and the rate is given by the Golden Rule expression^{10,41–44}

$$k_{\text{EnT}} = \frac{2\pi}{\hbar} V_{\text{TT}}^2 \text{FC}(T, \Delta E_{\text{EnT}}) \quad (6a)$$

where V_{TT} is the exchange coupling matrix element and $\text{FC}(T, \Delta E_{\text{EnT}})$ is the Franck–Condon weighted density of states, which describe the dependence of the rate on temperature, driving force, and vibrational modes that are coupled to energy transfer. The Franck–Condon term is given explicitly by eq 6b:^{18,43}

$$\text{FC}(T, \Delta E_{\text{EnT}}) = \sqrt{\frac{\pi}{\lambda_s k_{\text{B}} T}} \exp\{-(S^D + S^A)\} \sum_{w_i} \sum_{w_j} \frac{(S^D)^{w_i} (S^A)^{w_j}}{w_i! w_j!} \times \exp\left\{\frac{-(\Delta E_{\text{EnT}} + \lambda_s + w_i \hbar \omega_D + w_j \hbar \omega_A)}{4\lambda_s k_{\text{B}} T}\right\} \quad (6b)$$

where S^D (S^A) and $\hbar \omega_D$ ($\hbar \omega_A$) are, respectively, the unitless displacement and frequency of the dominant high-frequency mode that is displaced during energy transfer in the donor (acceptor), and λ_s is the sum of outer-sphere and low-frequency inner-sphere reorganization energies for de-excitation (excitation) of the donor (acceptor). The summations in eq 6b are taken over ground-state vibrational levels of the acceptor (w_i) and excited-state vibrational levels of the donor (w_j), and the other parameters have their usual meaning.

In the present study the Arrhenius equation was used to parametrize the temperature dependence of energy transfer,

$$k = A \exp\{-E_a/(RT)\} \quad (7)$$

where A is the frequency factor and E_a is the activation energy. Comparison of eqs 6 and 7 reveals that the frequency factor derived from an Arrhenius analysis is proportional to the exchange coupling matrix element in the quantum-mechanical expression (i.e., $A = CV_{\text{TT}}^2$, where C is a proportionality constant). Thus, the key to understanding the observation of the low-frequency factor for energy transfer in **2-ts**–**4-ts** lies in determining the origin of the low exchange coupling matrix element.

By application of eq 6, the experimental temperature-dependence data for **2-ts** was fitted to provide an estimate for V_{TT} . Figure 4 illustrates a plot comparing the experimental k_{EnT} data (markers) with rates calculated by using eq 6. In the calculation, the parameters used for the *trans*-stilbene acceptor ($S^A = 2$ and $\hbar \omega_A = 1300 \text{ cm}^{-1}$) were set equal to those determined in a study by Balzani and co-workers who fitted the dependence of k_{EnT} on ΔE_{EnT} for energy transfer from a variety of donors to *trans*-stilbene.⁴³ The parameters used for the bpy–Re chromophore ($S^D = 1$ and $\hbar \omega_D = 1300 \text{ cm}^{-1}$) are similar to those determined by emission spectral fitting.^{20,25} When these values are set to be constant and $\Delta E_{\text{EnT}} = -0.3$

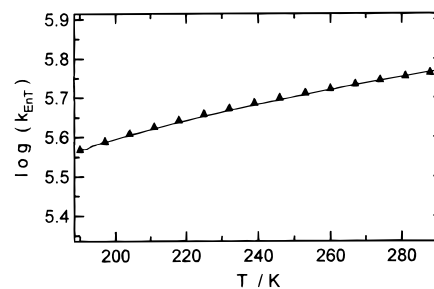


Figure 4. Plots of $\log(k_{\text{EnT}})$ vs T . Symbols mark experimental data for **2-ts** where k_{EnT} was calculated by using temperature-dependent τ_{em} data for **2-m** and **2-ts** in eq 2. Solid line is calculated by using eq 6 with parameters listed in text.

eV (-29 kJ mol^{-1}), the fit shown in Figure 4 was established by adjusting V_{TT} and λ_s . An optimal fit was obtained with $V_{\text{TT}} = 0.2 \text{ cm}^{-1}$ and $\lambda_s = 0.5 \text{ eV}$. Although there is some correlation between these two parameters in determining the fit, λ_s primarily influences the slope of the calculated line and V_{TT} is a “scaling” factor that moves the calculated line parallel to the vertical axis.

The value of $\lambda_s = 0.5 \text{ eV}$ determined by this fitting procedure is somewhat larger than one would anticipate. The primary contribution to λ_s is solvent polarization by the $^3d\pi^*$ state; temperature-dependent luminescence studies suggest that the contribution to λ_s due to solvent polarization is $\sim 0.25 \text{ eV}$.⁴⁵ However, λ_s also has a contribution from the stilbene chromophore that may amount to 0.15 eV . In any case, the value $V_{\text{TT}} = 0.2 \text{ cm}^{-1}$ determined by the fitting procedure is likely accurate to within $\pm 50\%$ and therefore provides a reasonable basis for comparison with values determined in other systems.

There are two possible reasons for the low apparent value of V_{TT} in **2-ts**. First, V_{TT} may be small because of the relatively large separation distance between the (diimine)Re donor and the *trans*-stilbene acceptor.⁴⁶ In the limit of weak donor–acceptor coupling, V_{TT} is proportional to the product of two overlap integrals for electronic wave functions localized on the energy donor and acceptor.^{41,47,48} Because it is proportional to orbital overlap, V_{TT} is strongly distance-dependent and decays exponentially with increasing donor–acceptor separation.^{47,48} A second plausible reason for the small V_{TT} is that energy transfer occurs by a nonvertical mechanism in **2-ts** (and by inference in **3-ts** and **4-ts** as well). Saltiel and co-workers observed low frequency factors⁴⁹ in their study of bimolecular endothermic energy transfer to *trans*-stilbene, which they attribute to poor Franck–Condon overlap arising from the requirement for twisting around the stilbene C=C bond in the transition state.^{9,10}

At this point we compare the V_{TT} value for **2-ts** to values determined for related systems in an effort to ascertain whether poor donor–acceptor coupling or nonvertical energy transfer is responsible for the low frequency factor. First, as noted above, Balzani and co-workers used eq 6 to model bimolecular energy transfer from a series of aromatic triplet donors to *cis*- and *trans*-stilbene and found that a value of $V_{\text{TT}} = 8 \text{ cm}^{-1}$ was required to fit the data.⁴³ This value is significantly larger than that for **2-ts**; however, electronic coupling is expected to be significantly larger in bimolecular systems because the donor and acceptor are unconstrained in the encounter complex and are able to come into proximity, thereby allowing good orbital overlap.

Cross and co-workers examined the driving-force dependence of intramolecular energy transfer from benzophenone to a series of triplet acceptors across a *cis*-1,4-cyclohexyl spacer.⁴⁴ Through

an analysis of the correlation of k_{EnT} with ΔE_{EnT} , they estimated that $V_{\text{TT}} = 0.3 \text{ cm}^{-1}$ in the 1,4-cyclohexyl-bridged system. An important observation is that the value of V_{TT} for the *cis*-1,4-cyclohexyl spacer is smaller by more than 2 orders of magnitude compared with the electronic coupling matrix element for electron (or hole) transfer across the same spacer ($V_{\text{el}} = 50 \text{ cm}^{-1}$).^{50,51} Closs and Miller delineated the relationship between V_{TT} and V_{el} and experimentally demonstrated that V_{TT} decays more sharply with distance than V_{el} .^{47,48,52} Thus, the fact that V_{TT} is dramatically lower than V_{el} for the 1,4-cyclohexyl spacer is consistent with the fact that V_{el} propagates better over long distance than V_{TT} .^{47,48}

Several electronic coupling factors are also available from our own work on intramolecular energy and electron transfer. First, in a study that examined highly exothermic energy transfer from the $^3d\pi^*$ state to the anthracene triplet in **1-A**, **2-A**, **4-A** and (and four other similar complexes), a value of $V_{\text{TT}} \approx 2 \text{ cm}^{-1}$ was determined by fitting the dependence of k_{EnT} on ΔE_{EnT} .¹⁸ Second, in a study of photoinduced electron transfer in **1-D**, **2-D**, and **4-D** (and three related complexes), a value of $V_{\text{el}} \approx 7 \text{ cm}^{-1}$ was determined by fitting the dependence of k_{ET} on ΔG_{ET} .¹⁷

Comparison of the V_{TT} value for **2-ts** with the V_{TT} and V_{el} values listed in the preceding paragraphs leads us to conclude that the low frequency factors for energy transfer in the Re–stilbene complexes arise solely because of weak electronic coupling between the energy donor and acceptor sites. Moreover, we conclude that (moderately endothermic) $\text{Re} \rightarrow \text{stilbene}$ energy transfer does not occur by a nonvertical pathway.⁵³ This point of view is developed on the basis of the following points. First, although V_{TT} in **2-ts** is lower than in the Re–anthracene system, in the latter the π -systems of the donor and acceptor are separated by two σ -bonds and in **2-ts** the π -systems are separated by four σ -bonds. On the basis of the Closs and Miller data, increasing the donor–acceptor separation from two to four σ -bonds will decrease V_{TT} by over factor of 10,^{47,48} consistent with the observed difference in the Re–stilbene and –anthracene systems.⁵⁴ A second, albeit less compelling argument, is based on the observation that V_{TT} for **2-ts** is more than 20 times lower than V_{el} for **1-D** (and the related series of complexes). This mirrors the factor of 150 difference between V_{el} and V_{TT} for the 1,4-cyclohexyl spacer system.^{44,50,51} Finally, in absolute terms V_{TT} is nearly the same for **2-ts** and for the 1,4-cyclohexane-bridged system.⁴⁴ This remarkable correspondence is in accord with the similar donor–acceptor separation distance in the two systems.

Summary

The photophysical and photochemical data indicate that intramolecular energy transfer from the diimine–Re chromophore to *trans*-stilbene occurs only when the process is moderately exothermic. Analysis of the temperature-dependent rate data reveals that moderately exothermic energy transfer is nearly activationless, consistent with a moderate outer-sphere reorganization energy ($\lambda_s \leq 0.5 \text{ eV}$). However, despite the fact that the driving force for energy transfer is nearly optimal in **2-ts–4-ts** (i.e., $\Delta E_{\text{EnT}} \approx \lambda$), the reaction is surprisingly slow. Slow energy transfer is attributed to poor electronic coupling between the diimine–Re donor and the *trans*-stilbene acceptor.

It is remarkable that energy transfer in **2-ts** is more than 100 times slower than photoinduced electron transfer in **2-D**, despite the fact that (1) the spacer is the same, (2) the driving force is similar, and (3) the reorganization energy for electron transfer

is nearly 2 times that for energy transfer. The large disparity in the rates of energy and electron transfer in the two (very similar) systems underscores the fact that the electronic coupling factor for energy transfer (V_{TT}) decays much more strongly with distance than that for electron transfer (V_{el}).

Acknowledgment. We gratefully acknowledge the National Science Foundation for support of this work (Grant No. CHE 94-01620). Megan Cooper and Osvaldo Sabina were participants in National Science Foundation Research Experiences for Undergraduates program (Grant No. CHE-9200344).

References and Notes

- (1) Saltiel, J.; Hammond, G. S. *J. Am. Chem. Soc.* **1963**, *85*, 2515.
- (2) Hammond, G. S.; Saltiel, J. *J. Am. Chem. Soc.* **1963**, *85*, 2516.
- (3) Herkstroeter, W. G.; Hammond, G. S. *J. Am. Chem. Soc.* **1966**, *88*, 4769.
- (4) Saltiel, J.; D'Agostino, J.; Megarity, E. D.; Metts, L.; Neuberger, K. R.; Wrighton, M. S.; Zafriou, O. C. *Org. Photochem.* **1973**, *3*, 1.
- (5) Gorman, A. A.; Beddoes, R. L.; Hamblett, S. P.; McNeeney, S. P.; Prescott, A. L.; Unett, D. J. *J. Chem. Soc., Chem. Commun.* **1991**, 963.
- (6) Forward, P. J.; Gorman, A. A.; Hamblett, I. J. *J. Chem. Soc., Chem. Commun.* **1993**, 250.
- (7) Gorman, A. A.; Hamblett, I.; Rushton, F. A. P.; Unett, D. J. *J. Chem. Soc., Chem. Commun.* **1993**, 983.
- (8) Gorman, A. A. *Spectrum* **1990**, *3*, 16–20.
- (9) Saltiel, J.; Charlton, J. L.; Mueller, W. B. *J. Am. Chem. Soc.* **1979**, *101*, 1347.
- (10) Saltiel, J.; Marchand, G. R.; Kirkor-Kaminska, E.; Smothers, W. K.; Mueller, W. B.; Charlton, J. L. *J. Am. Chem. Soc.* **1984**, *106*, 3144.
- (11) The Sandros equation, $k_{\text{EnT}} = k_{\text{diffusion}} \exp\{-\Delta E/(RT)\}$,¹² predicts that the rate of intermolecular endothermic energy transfer (k_{EnT}) will display an Arrhenius temperature dependence and that the observed activation energy will correspond to the difference in the spectroscopic triplet energies of the donor and acceptor (i.e., $E_{\text{act}} \approx \Delta E = E_{\text{acceptor}} - E_{\text{donor}}$).
- (12) Sandros, K. *Acta Chem. Scand.* **1964**, *18*, 2355.
- (13) Caldwell, R. A.; Riley, S. J.; Gorman, A. A.; McNeeney, S. P.; Unett, D. J. *J. Am. Chem. Soc.* **1992**, *114*, 4424.
- (14) Striplin, D. R.; Crosby, G. A. *J. Chem. Phys. Lett.* **1994**, *221*, 426.
- (15) Wrighton, M.; Morse, D. L. *J. Am. Chem. Soc.* **1974**, *96*, 998.
- (16) Giordano, P. J.; Wrighton, M. S. *J. Am. Chem. Soc.* **1979**, *101*, 2888.
- (17) MacQueen, D. B.; Schanze, K. S. *J. Am. Chem. Soc.* **1991**, *113*, 7470.
- (18) MacQueen, D. B.; Schanze, K. S. *J. Am. Chem. Soc.* **1992**, *114*, 1897.
- (19) Schanze, K. S.; MacQueen, D. B.; Perkins, T. A.; Cabana, L. A. *Coord. Chem. Rev.* **1993**, *122*, 63.
- (20) Wang, Y.; Schanze, K. S. *Inorg. Chem.* **1994**, *33*, 1354.
- (21) Boens, N.; DeRoock, T.; Dockx, J.; DeSchryver, F. C. *DECAN*, Version 1.0; 1991.
- (22) We use “imply” here because in order to confirm that the decrease in τ_{em} is due to an increase in k_{nr} , it is necessary to measure the emission quantum yield (ϕ_{em}) as well as τ_{em} . Emission yields were not determined in the course of the present study; however, in previous work with related Re(I) complexes we have confirmed that τ_{em} and ϕ_{em} decrease in parallel as $E_{\text{d}\pi^*}$ decreases.²⁰
- (23) Caspar, J. V.; Kober, E. M.; Sullivan, B. P.; Meyer, T. J. *J. Am. Chem. Soc.* **1982**, *104*, 630.
- (24) Caspar, J. V. Ph.D. Dissertation, University of North Carolina, Chapel Hill, NC, 1982.
- (25) Worl, L. A.; Duesing, R.; Chen, P.; Della Ciana, L.; Meyer, T. J. *J. Chem. Soc., Dalton Trans.* **1991**, 849.
- (26) Steady-state photochemistry to detect stilbene photoisomerization was not carried out on **4-ts** owing to overlap between the $d\pi^*$ and stilbene π,π^* absorption bands. Because of the overlap, it was not possible to selectively excite the $d\pi^*$ transition.
- (27) Görner, H.; Kuhn, H. *J. Adv. Photochem.* **1995**, *19*, 1.
- (28) Saltiel, J.; Khalil, G.-E.; Schanze, K. *J. Chem. Phys. Lett.* **1980**, *70*, 233.
- (29) Görner, H. *J. Phys. Chem.* **1989**, *93*, 1826.
- (30) Navon, G.; Sutin, N. *Inorg. Chem.* **1974**, *13*, 2159.
- (31) Song, X.; Endicott, J. F. *J. Chem. Phys. Lett.* **1993**, *204*, 400.
- (32) Hammond, G. S.; Saltiel, J.; Lamola, A. A.; Turro, N. J.; Bradshaw, J. S.; Cowan, D. O.; Counsell, R. C.; Vogt, V.; Dalton, C. *J. Am. Chem. Soc.* **1964**, *86*, 3197.
- (33) Saltiel, J.; Rousseau, A. D.; Thomas, B. *J. Am. Chem. Soc.* **1983**, *105*, 7631.

- (34) Görner, H.; Schulte-Frohlinde, D. *J. Phys. Chem.* **1981**, *85*, 1835.
- (35) Görner, H. *J. Chem. Soc., Faraday Trans.* **1993**, 4027.
- (36) Binstead, R. A. *SIMULATE*; University of North Carolina at Chapel Hill: NC, 1992.
- (37) Hager, G. D.; Crosby, G. A. *J. Am. Chem. Soc.* **1975**, *97*, 7031.
- (38) Caspar, J. V.; Kober, E. M.; Sullivan, B. P.; Meyer, T. J. *J. Am. Chem. Soc.* **1982**, *104*, 630.
- (39) Kober, E. M. Ph.D. Dissertation, University of North Carolina at Chapel Hill, 1982.
- (40) Ryu, C. K.; Schmehl, R. H. *J. Phys. Chem.* **1989**, *93*, 7961.
- (41) Dexter, D. L. *J. Chem. Phys.* **1953**, *21*, 866.
- (42) Scandola, F.; Balzani, V. *J. Chem. Educ.* **1983**, *60*, 814.
- (43) Orlandi, G.; Monti, S.; Barigelletti, F.; Balzani, V. *Chem. Phys.* **1980**, 313.
- (44) Sigman, M. E.; Closs, G. L. *J. Phys. Chem.* **1991**, *95*, 5012.
- (45) Lumpkin, R. S.; Meyer, T. J. *J. Phys. Chem.* **1986**, *90*, 5307.
- (46) The separation distance from Re to the center of the *trans*-stilbene chromophore is ~ 12 Å and four σ bonds intervene between the π -orbital systems of the two chromophores.
- (47) Closs, G. L.; Piotrowiak, P.; MacInnis, J. M.; Fleming, G. R. *J. Am. Chem. Soc.* **1988**, *110*, 2652.
- (48) Closs, G. L.; Johnson, M. D.; Miller, J. R.; Piotrowiak, P. *J. Am. Chem. Soc.* **1989**, *111*, 3751.
- (49) In the context of the present study, a low A value corresponds to a low "effective" V_{TT} . See ref 10 for an excellent discussion of the relationship between A , ΔS^\ddagger and V_{TT} .
- (50) Closs, G. L.; Calcaterra, L. T.; Green, N. J.; Penfield, K. W.; Miller, J. R. *J. Phys. Chem.* **1986**, *90*, 3673.
- (51) Closs, G. L.; Miller, J. R. *Science* **1988**, *240*, 440.
- (52) Theory and experiment demonstrate that V decays exponentially with distance according to the expression $V(r) = V^0 \exp\{-\beta(r - r_0)\}$, where $V(r)$ is the coupling for energy or electron transfer at donor-acceptor separation distance r , V^0 is the electronic coupling when the donor and acceptor are at separation distance r_0 (van der Waals contact), and β is a constant.^{50,51} Closs and Miller showed that $\beta_{TT} = 2\beta_{el}$, where the subscripts "TT" and "el" refer to triplet-triplet energy transfer and electron transfer, respectively.^{47,48}
- (53) The fact that energy transfer is vertical (i.e., *not nonvertical*) in **2-ts-4-ts** is not surprising given that energy transfer is moderately exothermic in these systems. Previous examples of nonvertical energy transfer involve systems in which energy transfer is endothermic.
- (54) A typical value of β_{TT} is 1.3 per bond;^{47,48} therefore, $V_{TT}(4 \text{ bonds}) \approx V_{TT}(2 \text{ bonds}) \times \exp\{-2.3\} = 0.07V_{TT}(2 \text{ bonds})$.